



Metabolic and Molecular Evidence for the Detection of the Pathogenic *Pseudomonas aeruginosa* on Common Bean Seeds and Its Control Via Chitosan-silver Nanocomposite



Marwa S. Fouad^{(1)#}, WesamEldin I.A. Saber^{(2)#}, Huda H. Badr⁽³⁾, Hisham A. Mohamed⁽¹⁾, Khaled Y. Farroh⁽⁴⁾, Ahmed A. Gomah⁽³⁾

⁽¹⁾Seed Pathology Research Department, Plant Pathology Research Institute, Agricultural Research Centre, Giza 58312, Egypt; ⁽²⁾Microbial Activity Unit, Microbiology Department, Soils, Water and Environment Research Institute, Agricultural Research Centre, Giza 12619, Egypt; ⁽³⁾Bacterial Diseases Research Department, Plant Pathology Research Institute, Agricultural Research Centre, Giza 58312, Egypt; ⁽⁴⁾Nanotechnology and Advanced Materials Central Lab, Agricultural Research Centre, Giza 58312, Egypt.

THE CURRENT study stated the novel pathogenic action of *Pseudomonas aeruginosa* MA1 on common bean, causing the soft rot of seeds as the infection route. The pathogenic bacterium was molecularly identified and deposited in NCBI GenBank with an accession number of ON000399. Enzymatic activities of xylanase, cellulase, pectinase, proteinase and protease were observed to be 13.054, 11.09, 9.28, 20.90, and 1.47U respectively, indicating the ability of MA1 to invade the plant tissue, recording a disease incidence of 63.25% with a severity of 42.52%. The physiological features showed a remarkable decrease in chlorophyll content with an increase in proline and phenolic contents in the infected plant. Both peroxidase and phenylalanine ammonia-lyase (PAL) activities increased, reaching their maximum value after 72h of infection with a significant overexpression of the PAL gene after 24h. that proves the pathogenic role of *P. aeruginosa* on common bean. However, seed transmission is paramount in further pathological studies since the current pathogenic bacterium was detected on seeds. *In-vitro* evaluation of the chitosan-silver nanocomposite (Ch-Ag NC) reveals the first management protocol for the bacterial pathogen MA1 that was confirmed by applying (Ch-Ag NC) in the greenhouse. Furthermore, *in-situ* application of Ch-Ag NC (50 and 100mg/L) suppressed bacterial infection with a significant increase in seedling growth properties.

Keywords: Defense-related enzymes, Disease management, Lytic enzymes, PAL gene, *Pseudomonas aeruginosa*, Seed germination.

Introduction

Common bean, or French bean (*Phaseolus vulgaris* L.), is an essential legume worldwide for the edibility of dry seeds and mature fruits. According to Food and Agricultural Organization Statistics (FAO, 2020), the total world yield of dry beans, mainly from Myanmar, India, Brazil, China, Mexico, Tanzania, and the USA, was 27.5 million metric tons in 2020, harvested from 34.8 million hectares. According to the Egyptian Ministry of Agriculture Statistics, the area devoted to dry seeds was about 8850 hectares, yielding about

29634 metric tons, with an average of 3.18 metric tons/hectare. The protein-rich seed is an excellent substitute for animal protein and is therefore considered an alternative to meat in developing countries. In addition, the leaf is also used as a vegetable and the straw as fodder (Moghazy, 2014). Being a member of the leguminous family Fabaceae, *Phaseolus* species are distinguished by their ability to hold atmospheric nitrogen through the symbiotic relationship between their roots and the nitrogen-fixing bacteria rhizobia (Peralta et al., 2016).

#Corresponding authors emails: msfouad2020@yahoo.com (M.F); wesameldin.saber@arc.sci.eg (W.S.)

Tel.: +20- 0111 173 1062 (W.S.); +20- 01203770990 (M.F)

Received 19/05/2023; Accepted 31/10/2023

DOI: 10.21608/ejbo.2023.212107.2337

Edited by: Prof. Dr. Rashad Younes, City of Scientific Research and Technological Applications, Alexandria, Egypt.

©2024 National Information and Documentation Center (NIDOC)

Depending on soil type, the associated microbiome analysis revealed a plethora of pathogenic *Pseudomonas* (Chiniqy et al., 2021), affecting common bean. *Pseudomonas* spp. are non-spore-forming, rod-shaped, Gram-negative, and oxidase-positive bacteria (Young & Park, 2007). Phytopathogenic *Pseudomonas* is widely distributed in plants, causing pronounced plant problems (Walker et al., 2004; Moore et al., 2013). The important bean seed-transmitted bacteria are *Pseudomonas savastanoi* pv. *phaseolicola* which causes halo blight disease, and *Pseudomonas savastanoi* pv. *syringae*, which causes bacterial brown spot disease. Primary sources of infection with *P. s.* pv. *phaseolicola* include internally or externally contaminated seeds, and given the right environmental conditions, even very small amounts of inoculum can cause catastrophic epidemics. After the initial infection with *P. s.* pv. *Syringae*, the symptoms of young halo blight are similar to the bacterial brown spot, and small water-soaked spots were noticed on the underside of new foliage. When a lesion reaches maturity, it typically takes on the appearance of a brown spot and any dead tissue in the center may fall out giving the lesion of a shot-hole appearance. Contaminated seed is the main source of inoculum, and to stop the spread of disease, it is crucial to produce pathogen-free certified seed (Popovic et al., 2012; Boersma et al., 2014; Chatterton et al., 2016).

A certain isolate of *Pseudomonas aeruginosa* is a phytopathogenic bacterium that causes leaf spots in lettuce (Cortes-Monllor, 1993). Also, *P. aeruginosa* was isolated from the onion bulb with soft rot disease (Abd-Alla et al., 2011). Such a disease leads to a severe loss in vegetable and ornamental yield worldwide (Emami et al., 2018), and some strains of this bacteria may be potent opportunistic human/animal pathogens (Tuon et al., 2022). Moreover, Chahtane et al. (2018) documented the germination-arresting effect of *P. aeruginosa* on *Arabidopsis*. However, no previous reports show that *P. aeruginosa* causes soft rot disease in common bean.

Chitosan is relatively cheap and considered the second most abundant natural biopolymer. Different theories elucidate the antimicrobial properties that can be enhanced by transformation into chitosan nanocomposites, to increase their temperature stability and lower their volatility (Kumar & Münstedt, 2005; Feng et al., 2013).

One of these hypotheses is called “intracellular leakage,” where the positively charged chitosan attaches to the negatively charged molecules on bacterial surfaces like lipopolysaccharides. Due to this binding, the permeability of the bacterial membrane changes, resulting in the release of intracellular constituents and cell death. Compared to chitosan alone, chitosan nanoparticles (C NPs) demonstrated better antibacterial activity against a variety of Gram-positive and Gram-negative bacteria, which implies that CNPs may have the ability to function as an antibacterial agent (Alqahtani et al., 2020). Additionally, it was reported that chitosan was recommended as a good stabilizer for silver nanoparticles (AgNPs). Furthermore, chitosan-silver nanocomposite exhibits great efficiency in killing bacteria and fungi (Wang et al., 2015).

The present research aims to evaluate the pathogenicity of the seed-transmitted bacterial pathogen *P. aeruginosa* on common bean. In addition, the defense-related mechanisms associated with common bean infection were assessed to measure the host’s metabolic changes, including the determination of peroxidase (POX) and PAL activity that proceeded by accumulating PAL mRNA transcripts. Furthermore, we observed the antimicrobial activity of chitosan-silver nanocomposite against *P. aeruginosa* as a potential control strategy for the pathogen.

Materials and Methods

Common bean seeds

Seeds of *Phaseolus vulgaris* L. (Paulista cultivar; Dutch in origin and winter crop) were obtained from the Central Administration for Seed Production (CASP), Ministry of Agriculture, Giza, Egypt.

Isolation of the pathogenic bacterium

A direct detection method for bacterial diseases in growing seeds followed the recommended methods from the International Seed Pathology Association (ISTA, 2007). Seeds of *Phaseolus vulgaris* were surface sterilized by submerging them in 2% sodium hypochlorite for 3 minutes. Then, the seeds were washed several times with sterilized water and left to dry using sterilized filter paper. In the greenhouse, seeds were introduced to pots containing disinfested soil (Sand: Patmos at 1:1 v/v). Three seeds were seeded per pot for seedling inspection.

Under septic conditions, the diseased parts of the emerging seedlings were cut into small pieces and immersed in 1 ml of a sterilized saline phosphate buffer (pH 7). Serial dilutions were prepared from the previous suspension, spread on King's B medium (KB) (King et al., 1954), and incubated at $28 \pm 2^\circ\text{C}$ for 24 h. Single colonies were picked up and purified, then retained on KB slants for identification and further tests.

Pathogenicity test of isolated bacteria

All greenhouse experiments were conducted at the Agricultural Research Centre, Giza, Egypt (latitude: $30^\circ 01' 16.99''$ N and longitude: $31^\circ 12' 30.01''$ E). A pathogenicity test for the isolated bacterium was carried out in the greenhouse using pots containing 3 kg/pot of disinfected soil (Sand: Clay at 1: 2 v/v). Precisely, three pre-surface sterilizing seeds (by submerging in 2% sodium hypochlorite for ten minutes and washing many times with sterile water) of common bean were seeded per pot. In addition, the bacterial inoculum was grown on KB broth medium for 24 h at $28 \pm 2^\circ\text{C}$. Pathogenicity test was carried out following detached pod and infesting leaf methods as non-destructive and inexpensive methods as the following description:

Pathogenicity test on detached common bean pods

Under aseptic conditions, the pathogenicity test of bean pods protocol was carried out according to the method designated by Hepperly & Sinclair (1980); detached healthy bean pods with full-sized beans were surface sterilized with 70% ethyl alcohol for 2min. Precisely, $100\mu\text{L}$ of 10^6 cfu/mL for the isolated bacterial inoculum was injected into sterilizing healthy detached bean pods in holes of 2 mm diameter. Pods were incubated at $28 \pm 2^\circ\text{C}$ for 3-4 days. The presence of soft rot symptoms (a water-soaking area) or a hypersensitive reaction at the stab inoculation site was considered a result of the pathogenicity testing. The pathogenic bacteria were re-isolated from the diseased parts of infected pods and re-cultured on KB slants.

Pathogenicity test on common bean leaves

Pathogenicity test of isolated bacteria was determined by making minor wounds on the surface of sterilized healthy leaves for common bean seedlings 25-30 days old by scratching with carborundum powder, and each isolated bacterial suspension was sprayed at 10^6 cfu/ml of 24h-old

culture. Distilled sterilized water was used in the control pots instead of the bacterial suspension. Artificially infected seedlings were covered with plastic bags for 24h to increase the humidity level (Zaiter & Coyne, 1984). Seedlings were irrigated with tap water only. The symptoms that appeared developed and scored five days' post-inoculation. Disease incidence (DI) was assessed as the presence or absence of disease (percentage of infected plants) according to the following equation:

$$\text{DI (\%)} = \left(\frac{\text{Number of infected plants}}{\text{Total assessed plants}} \right) \times 100$$

The severity was rated according to the percentage of yellowish-brown or necrotic area in the leaf with a progression scale from 0 to 4, where 0 = 0%; 1= 1- 25%; 2= 25 -50%; 3= 50 - 75% and 4= 75 -100%. Then the disease severity (DS) was calculated according to the following equation:

$$\text{DS (\%)} = \left(\frac{\sum(nV)}{4N} \right) \times 100$$

where: n= the number of leaves in each category, V= the numerical values of the symptoms category, (N) = the total number of leaves, and (4)= the maximum numerical value of the symptom category (Waller et al., 2002).

Effect of pathogenic bacterium against seed germination rate and vigor index

The effect of the purified isolated bacterium on seed germination and vigor index was tested fifteen days after seed sowing. The surface of common bean seeds was sterilized as mentioned earlier then washed well with sterile water and desiccated using filter paper. The surface disinfected seeds were immersed in the bacterial suspension with different cell densities of (10^2 , 10^6 , and 10^{10} cfu/mL) and incubated at $28 \pm 2^\circ\text{C}$ for 6h in the presence of an Arabic gum to confirm the assembly of bacterial cells on the seed surface and allow them to air dry. Three seeds were sowed per pot of disinfected soil (sand: clay at 1:2 v/v). Sterilized water was used in control pots instead of bacterial suspension (Garge et al., 2018). After fifteen days, the germination percentage and growth parameters including shoot, root lengths and the number of rootlets were determined. To assess the impact of the tested bacteria on seed germination and seedling growth properties, the germination rate (%) and the vigor index,

respectively, were calculated according to the following equations reported by Masum et al. (2012):

$$\text{Germination rate} = \left(\frac{\text{number of healthy seedlings}}{\text{total number of seeds}} \right) \times 100.$$

$$\text{Vigor index (I)} = \text{Germination (\%)} \times \text{seedling length (root + shoot)}$$

Bacterial identification

Phenotypic characteristics and biochemical tests

The bacterial isolate was identified based on its phenotypic characteristics, such as motility, colony morphology, cell shape, and enzymatic hydrolytic activity. Also, biochemical tests (Gram staining, fluorescent pigment on KB medium under UV light, cytochrome oxidase test, KOH test, catalase activity, starch, and gelatin hydrolysis) were considered (Garrity et al., 2005; Cartwright, 2010).

Molecular identification

DNA was extracted from the pathogenic bacterial cells using sodium dodecyl sulphate (Zhou et al., 1996). A pure 24-h-old bacterial colony was suspended in 100 µl of lysis solution (0.05 M NaOH, 0.25% sodium dodecyl sulphate) and incubated for 15 minutes at 100°C., then centrifuged (1min at 12,000rpm). The pellets were discarded.

In sterile distilled water, the DNA suspension was diluted 50 times. The reaction mixture involved 5 µl of the diluted suspension with forward and reverse primers 27F (AGAGTTTGATCCTGGCTCAG) and 1492R (GGTACCTTGTTACGACTT), respectively. The 16S rRNA gene was amplified from the isolated genomic DNA (Polz & Cavanaugh, 1998).

The PCR amplification for the 16S rRNA gene was to a near-full length, almost 1500 bp fragment. The PCR amplification protocol was carried out in a 50 µl reaction volume, counting; Dream Taq Green PCR Master Mix (2X) (25µL), forward primer (2µL), reverse primer (2µL), Template DNA (4µL), and water, nuclease-free (17µL), then the sample was gently vortexed and spun down.

The PCR thermal cycling conditions were

initial denaturation (one cycle at 95°C for 5min), denaturation (40 cycles at 95°C for 30sec), annealing (40 cycles at 56°C for 30sec), extension (40 cycles at 72°C for 30sec), and final extension (on the final cycle at 72°C for 10min). The PCR product was purified, and the sequence was read through the MacroGen Sequencing Order System. The 16S rRNA gene sequence was aligned with the corresponding sequences on the databases of GenBank by using the BLAST tool. The evolutionary relationships were constructed using the Neighbor-Joining technique (Saitou & Nei, 1987). The percentage of replicate trees in the related taxa was estimated (Felsenstein, 1985). The vague points were removed for each sequence pair by the pairwise deletion method. MEGA11 was used (Tamura et al., 2021).

Hydrolytic activity

Culturing technique

The solid-state fermentation (SSF) procedure was applied to screen the bacterium for various enzymes. The dried plant was ground and used as a substrate in the fermentation medium to simulate the natural environmental conditions of the bacterium. One gram of dried plants was mixed with tap water (5mL, pH 7.2) in 250mL Erlenmeyer flasks and autoclaved (121°C for 15min), then injected with 1.0mL of 10⁶ cfu/mL, which was previously prepared from a 2-days-old culture grown on a nutrient broth medium. The medium moisture was kept constant by adding sterilized water when needed. After ten days of incubation (30°C), the grown culture was mixed with 10 mL of Tween 80 and shaken (150 rpm for 30min) on a rotary shaker. The bacterial supernatant was separated by filtration (using Whatman No. 1 filter paper), centrifugation (4100 xg for 20min), and assayed for lytic enzymes.

Enzyme's assay

Xylanase and cellulase were assayed utilizing xylan, and microcrystalline cellulose as substrates, respectively. 0.5% of the substrate was dissolved in citrate buffer (0.05 M, pH 4.8) and mixed with 1 ml of the filtrate. The mixture was incubated at 50 °C for 30 min for xylanase and 60 min for cellulase (Saber et al., 2010). After incubation time, the released reducing groups were detected (Bailey et al., 1992). The unit (U) of the xylanase or cellulase was defined as the enzyme amount needed to liberate one µmol/g/min of xylose (xylanase) or glucose (cellulase) under the assay conditions.

The catalytic action of polygalacturonase (pectinase) was assayed in the bacterial supernatant mixed with sodium acetate buffer (0.1 M, pH 5.2). The released polygalacturonic acid groups after 30min incubation at 40°C were determined (Ajayi et al., 2021). The “U” of pectinase was the amount that released 1.0µmol/g/min of polygalacturonic acid under the assay conditions.

The quantitative proteolysis activity (protease) was tested in a mixture of supernatant and casein substrate. The free amino acids separated after incubation (37°C for 10min) were determined at 280. Under the test conditions, one protease unit was identified as the enzyme amount liberating 1.0 µg equivalent of tyrosine, as standard, /min. tyrosine was measured at different concentrations at 280 (Al-Askar et al., 2022a).

Lipase activity was determined in a mixture of olive oil emulsion, 0.2 M Tris HCl buffer (pH 7.5), and enzyme solution. The tubes containing reaction mixtures were incubated in a reciprocating shaking water bath at 40°C for 10 min. The liberated free fatty acid total was titrated against 0.01 N NaOH (Saber, 2004). One unit of lipase was identified as the quantity of enzyme required to liberate 1.0µ mol of fatty acids per minute under the experimental conditions.

Metabolic changes in common beans

The phenolic (total and free) content of common bean was determined in the leaves of infected and healthy plants using a spectrophotometer (UV-Vis Spectronic 601). The density of the blue color developed was measured at 520 nm using catechol as standard (Snell & Snell, 1953). The colorimetric ninhydrin method was utilized to measure proline content (Bates et al., 1973). Total chlorophyll content was evaluated according to Dere et al. (1998).

Defense-related enzymes

Peroxidase (POX) and phenylalanine ammonia-lyase (PAL) activities were determined in the leaves of healthy and infected common bean plants for 5 days after infection.

Peroxidase assay

Peroxidase enzyme activity was determined as described by Seevers et al., (1971). Leaf tissue was homogenized in sodium acetate buffer (0.1 N, pH 5.0) in a 1:10 ratio (g/mL) and the homogenate was centrifuged at 20000 *xg* for 20min. Crude

enzyme extract was diluted with acetate buffer, and an equivalent volume of sod. acetate buffer (pH 5.0) was substituted for H₂O₂ in the reference cuvette in the control assay. The diluted enzyme extract was used in the colorimetric determination of peroxidase activity for 5 minutes at 25°C using a wavelength of 470 nm for O.dianisidine as a substrate. The reaction mixture consists of 1.8 ml of 20mM sod. acetate buffer (pH 5.0); 0.05 ml of O.dianisidine (1% in absolute methanol); 0.2 ml of 30mM H₂O₂, and 0.1 ml of enzyme solution. One unit of the enzyme activity was identified as an increase in optical density (OD = 0.1 per min./gram fresh weight) (Seleim et al., 2014).

PAL assay

PAL enzyme activity was determined by measuring the trans-cinnamic acid formation rate in treated common bean leaves (Zucker, 1965). PAL activity was determined by measuring the rate of formation of trans-cinnamic acid in leaf tissue. In a 1:10 ratio, leaf tissue was homogenized in borate buffer (25mM, pH 8.8) containing 20mM 2-mercaptoethanol. The homogenate was centrifuged at 20000 *xg* at 2°C for 10min, and the resulting supernatant was used as enzyme preparation. The reaction mixture contained 33mM sodium borate buffer (pH 8.8), 10mM of L-phenylalanine, and 0.2mL enzyme extract in a total volume of 3mL. The amount of cinnamic acid during one hour at 37°C, was calculated through the increase in absorbance at 290nm. One PAL unit was identified as an increase in optical density (OD = 0.1 per h./gram fresh weight).

Assessment of the molecular defense-related mechanism of PAL transcripts

The molecular defense-related mechanism was assessed by expressing the PAL gene in healthy and infected leaves (Kohler et al., 2002) after 1, 3, and 5 days of infection. Thermo Scientific GeneJET RNA purification kits (0731, 0732) were used for RNA isolation. A NanoDrop spectrophotometer (ND 2000c, ThermoFisherScientific, Wilmington, DE, USA) was used to confirm RNA purity and concentration. The cDNA was synthesized using 1 µg RNA using the Thermo Scientific RevertAid First Strand cDNA synthesis kit (1621, 1622) following the standard protocol from the manufacturer. With the specific primers: 5'-AAGCACCACCCTGGTCAAATTGAG-3' and 5'-GACAAGCTCGGAGAATTGAGCAAAC-3' and using the Mx3000P (Stratagene, CA, USA) qPCRsystem,quantitativeamplificationsofthePAL

gene were performed. Results were normalized to those of actin as endogenous control using the primers 5'- GTTCCCTGGTATTGCGGACA -3' and 5'- TTTTCTATCGCCGACCCAC -3'. The thermal cycler program was initial denaturation at 95°C for 10min, followed by 40 two-step cycles of amplification (95 °C for 15sec and 60°C for 60sec). The average expression recorded in the non-infected leaves was considered a quantification unit.

Control of P. aeruginosa MA1 using chitosan-silver nanocomposite

Preparation of chitosan-silver nanocomposite

The chitosan reduction of silver nitrate produced the chitosan-silver nanocomposite (Ch-Ag NC) (Babu et al., 2017). In an acidic solution of chitosan, polymeric chains' amino groups coordinate the silver ion. Metallic silver nanoparticles are created when the hydroxyl group in chitosan is oxidized and coupled with ion reduction. In brief, chitosan was dissolved in an acetic acid solution (1% v/v) (99-100%, Riedel-de Haan) at room temperature to create chitosan aqueous solution (1% w/v) (molecular weight 50 – 190kDa, degree of deacetylation 75–85%, and viscosity: 20–300 cP, Sigma-Aldrich, USA). After that, the solution was immediately mixed with the silver nitrate solution (0.01M) (Sigma-Aldrich, USA) while being stirred for two hours. The preceding suspension had a rapid color shift from pale yellow to brown after the addition of sodium borohydride (20mL, 0.04M) (Sigma-Aldrich, USA). The resulting chitosan-silver nanocomposite suspension was centrifuged (20000 xg, 30min). Before being used or analyzed, the Ch-Ag NC pellets were resuspended in deionized water and then frozen.

Characterization of Ch-Ag NC

The chitosan-silver nanoparticles' size (Z-average mean) and zeta potential were measured in triplicate using a Zeta sizer 3000HS (Malvern Instruments, ZS Nano, UK) by photon correlation spectroscopy and laser Doppler anemometry, respectively. The high-resolution transmission electron microscope (HR-TEM) (Tecnai G2, FEI, Netherlands) was used to image the actual morphology of the Ch-Ag NC as it had been formed. To lessen particle aggregation, the diluted Ch-Ag NC solution was ultrasonically sonicated for 5 min. Three drops of the sonicated solution were applied with a micropipette to a copper grid that had been coated with carbon, and

the grid was left to air dry at room temperature. For morphological analysis, HR-TEM pictures of the Ch-Ag NC that had been deposited on the grid were taken. Using the X-ray Diffraction (XRD) technique, the chemical structure of Ch-Ag NC as it had been produced was evaluated. In the scanning mode of an X-ray diffractometer (X'pert PRO, PAN analytical, Netherlands) using a Cu K radiation tube (= 1.54Å) operating at 40kV and 30 mA, the appropriate XRD pattern was captured. The standard ICCD library built into the PDF4 software was used to analyze the acquired diffraction pattern. An Inductivity-Coupled Plasma (ICP) technology (PerkinElmer ICP-OES: Optima 2000, Germany) was used to quantify the applied silver concentrations in Ch-Ag NC both qualitatively and quantitatively. The FTIR (IR-affinity INVENIOS-BRUKER spectrometer) was used to evaluate functional group confirmations. Fourier transform infrared spectroscopy (FTIR) analysis was used to characterize the presence of molecular bonds during the formation of the Ch-Ag NC, and this information was subsequently required to approve the identity of the chitosan-silver nanocomposite. The material was analyzed by performing 10 scans on the spectrum with a resolution of 0.1cm⁻¹, ranging from 400 to 4000cm⁻¹ for each scan.

In-vitro antibacterial activity of Ch-Ag NC

In acetic acid (1%), Ch-Ag NC, several concentrations (5, 10, 20, 30, 40, 50, and 100mg/L) were produced. Acetic acid (1%) was used as a control. Agar-well diffusion assay was used. King B medium was poured into Petri plates (9 cm in diameter) and allowed to solidify. MA1 was spread on the medium surface, and wells (5mm) were cut in the solid medium using a sterile cork borer. Wells were filled individually with 100µL of each concentration, and the plates were left at 4-5°C overnight to allow the diffusion of Ch-Ag NC and stop bacterial growth. Then, the plates were incubated at 30°C. After a 24- hour incubation period, the diameter of the inhibition zone around the well was measured using a calibrated ruler and compared to acetic acid at 1% (Wolf & Gibbones, 1996).

In-vivo application of Ch-Ag NC for controlling P. aeruginosa infection in greenhouse

Common bean seeds were surface sterilized as mentioned in pathogenicity test and then the sterilized seeds were dipped in Ch-Ag NC solutions of 50 and 100mg/L individually for

three hours for coating. Arabic gum was added to ensure the adhesion of nanoparticles to the seed surface and allow them to air dry. The coated seeds were divided into two groups; the first group was introduced to soil (sand: clay at 1:2 v/v) inoculated with the tested bacteria, and it could be ensured that the bacterial count in the soil was 10^6 cfu/mL. The other group was introduced to disinfected soil without any bacterial inoculation (to study the effect of nanoparticles on seedling growth properties as a positive control). Uncoated, sterilized seeds were used in pots without any treatment, acting as a negative control. Three seeds were seeded per pot. Growth parameters, including shoots, root lengths, and the number of rootlets, were measured to assess the antibacterial activity of Ch-Ag NC on the tested bacteria.

Statistical analysis

The data were presented as the mean \pm standard deviation (SD). Germination and pathogenicity test data were analyzed using a one-way ANOVA. T-test procedures were used for two samples' comparison and the Tukey–Kramer test for multiple comparisons. The 0.05 level of probability was used as the significance level. The statistical software MINITAB (Minitab® 19.2020.1 version, Minitab Inc., State College, PA, USA) was used.

Results

Isolation and pathogenicity test of the isolated bacteria

Bacterial isolate obtained from bean seedlings on KB medium gave the same symptoms of soft rot (water soaking) in growing seedlings (Fig. 1, A) and produced blue-green pigment on KB medium. Pathogenicity was confirmed through Kock's postulates in bean pods for the bacterial isolate that gave the same symptoms (Fig. 1, B). A confirmed pathogenicity test was carried out on bean leaves in the greenhouse using a foliar spray of the bacterial suspension showed a remarkable ability to develop infection symptoms after five days of inoculation, displaying characteristic chlorotic lesions with brown necrotic edges around the site of infection (Fig. 1, C). Bacterial infection was assessed, recording a disease incidence of 63.25% with a severity of 42.52% (Table 1).

Effect of pathogenic bacterium against

germination (percentage and rate) and vigor index

The germination percentage was not affected significantly by the lowest bacterial cell density of 10^2 cfu/mL, but it decreased with the further increase in bacterial cell densities, reaching 26.47% at 10^{10} cfu/ml compared to the control. The shoot length showed a significant gradual decrease with the increase in bacterial cell density, reaching 48.18% of control at 10^6 cfu/ml. The further increase in bacterial cell density was accompanied by complete inhibition of shoot emergence, and germination was restricted to the appearance of a small radicle, or development of very stunting seedlings as shown in Fig. 2. Additionally, root length and the number of rootlets decreased gradually with the increase in bacterial cell density, showing the complete absence of rootlets with a bacterial inoculum of 10^{10} cfu/mL. Consequently, increasing *P. aeruginosa* inoculum densities caused a significant reduction in both germination rate by (5.88, 23.52 and 76.47%) and vigor index by (22.12, 61.05, and 97.8%) for 10^2 , 10^6 , and 10^{10} bacterial inoculum densities, respectively compared to control (Table 2).

Bacterial identification

The isolated pathogenic bacterium had phenotypic characteristics of non-spore-forming, motile, and tiny rod-shaped cells. In addition, when it was grown on KB medium, it had the shape of tiny circular colonies and a secret fluorescent pigment. It can solubilize KOH and is a Gram-negative bacterium. The enzymatic activity showed positive action for catalase and starch hydrolysis, whereas it was negative for cytochrome oxidase and gelatin hydrolysis. Accordingly, the phenotypic and biochemical tests revealed that the pathogenic bacterium was classified as *Pseudomonas* spp.

Molecular classification

The bacterial isolate MA1 was molecularly identified. From the blast data of the GenBank, the isolated strain MA1 showed a similarity with *P. aeruginosa* (Fig. 3). The percentage of replicate trees that clustered similar bacteria together in the bootstrap test (involving 18 nucleotide sequences) is shown above the branches. Accordingly, the strain MA1 was identified and classified as Proteobacteria, Gammaproteobacteria, Pseudomonadales, Pseudomonadaceae, and *P. aeruginosa* strain MA1. Consequently, the Gen Bank accession number was received as ON000399.

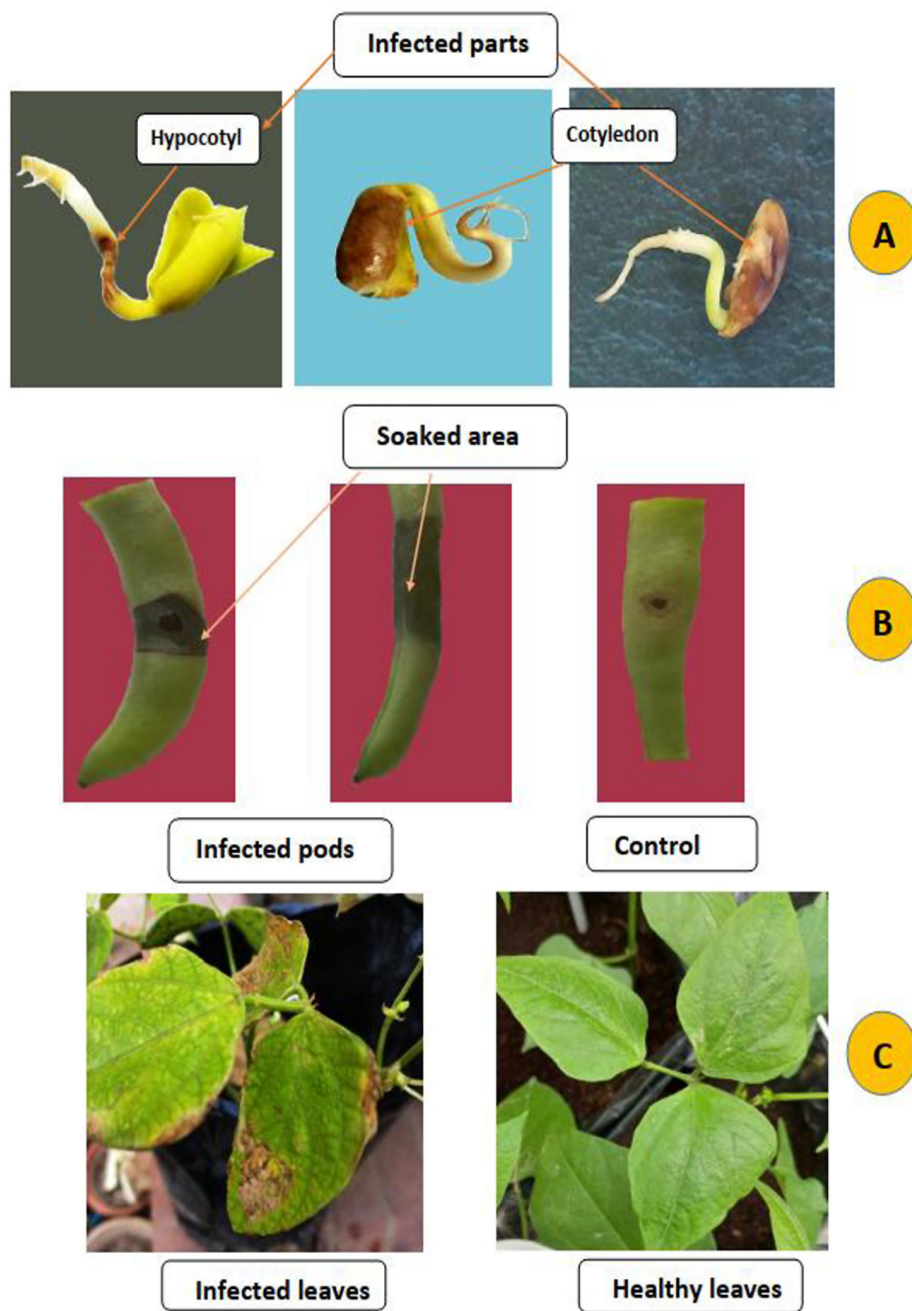


Fig. 1. Soft rot symptoms in naturally infected cotyledons and hypocotyl (A), Symptoms of artificial bacterial infection in bean pods (B) and characteristic chlorotic lesions in artificially infected leaves (C)

TABLE 1. Assessment of leaf spot symptoms caused by *P. aeruginosa* on common bean plants

Treatment	Disease Incidence % (DI)	Disease severity % (DS)
Non-infected control	0.0±0.0 b	0.0±0.0 b
Infected plant	63.25±6.86 a	42.52±5.33 a

The Values were represented as mean ± SD, n= 10.

The means of the same parameter with different letters are significantly different (T-test at $P \leq 0.05$).

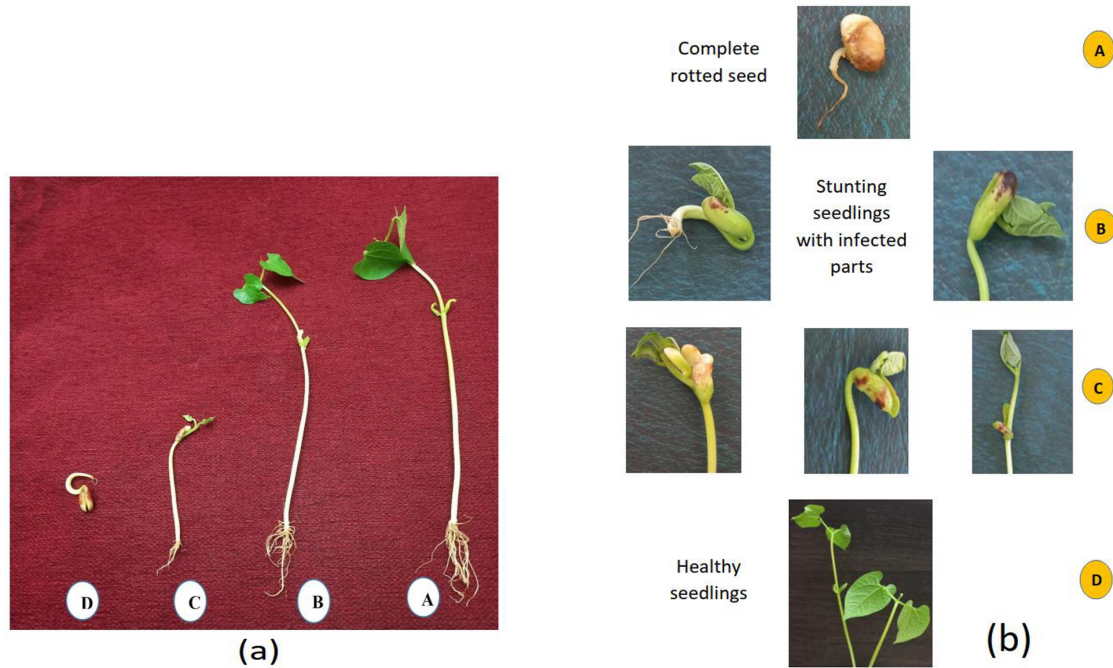


Fig. 2. (a). Effect of different *P. aeruginosa* cell densities on germination rate: (A): Control; (B): 10^2 cfu/mL; (C): 10^6 cfu/mL; (D): 10^{10} cfu/mL. (b): Magnified image showing infected parts and seedling size under the effect of different cell densities of *P. aeruginosa*, (A): 10^{10} cfu/mL; (B): 10^6 cfu/mL; (C): 10^2 cfu/mL; (D): control

TABLE 2. Effect of bacterial cell densities on the emerging seedling’s relative germination and vigor index

Bacterial cell density (cfu/mL)	Shoot length (cm)	Root length (cm)	Number of rootlets	Germination (%)	Germination rate (%)	Vigor Index
Control	16.85 ± 1.12 a	5.03 ± 0.46 a	13.00±1.01 a	94.44±13.61 a	94.44 ± 13.61 a	2066.00 ± 340.00 a
10^2	14.58 ± 1.59 b	3.52 ± 0.28 b	10.89±0.49 b	94.45± 13.61 a	88.89 ± 17.21 ab	1609.00 ± 381.00 b
10^6	8.12 ± 2.02 c	3.02 ± 0.28 c	7.00±0.67 c	77.78±1721 b	72.23 ± 13.61 b	804.64 ± 179.20 c
10^{10}	0.00 ± 0.00 d	2.05 ± 0.19 d	0.00±0.00 d	25.00± 20.41 c	22.22 ± 17.21 c	45.55 ± 34.30 d

Values were represented as mean ± SD, n=6.

The means of the same parameter with different letters are significantly different (Tukey test at $P \leq 0.05$).

Lytic activity of the isolated bacterial pathogen on common bean plant tissue

The lytic activity of the cultural supernatant of the bacterial pathogen was discovered (Fig. 4). The enzyme activity varied accordingly, being 13.054, 11.09, 9.28, 20.90, and 1.47 U for xylanase, cellulase, pectinase, proteinase, and lipase, respectively. Additionally, the pH of the cultural supernatant was found to be in the neutral range (7.27).

Metabolic changes in common beans

Metabolic changes in the leaf tissue of the infected plants displayed a decrease in chlorophyll b and total chlorophyll contents by 24.33 and 34.27%, respectively, compared to the control. On the other

hand, total carotenoids, proline, and phenolic compounds (total and free) increased in infected plant by 103.65, 183.33, 119.38, and 133.38% respectively, in relation to non-infected plants (Table 3).

Defense-related enzymes

The time profile of POX and PAL in the common bean plant was followed up for five days as a response to infection by *P. aeruginosa*. Both enzymes exhibited almost the same pattern (Fig. 5, a, b), in which POX and PAL increased significantly, reaching their peak activity on the third day of infection at 5061.3 and 117.63 U/g fresh weight, respectively, and then declined.

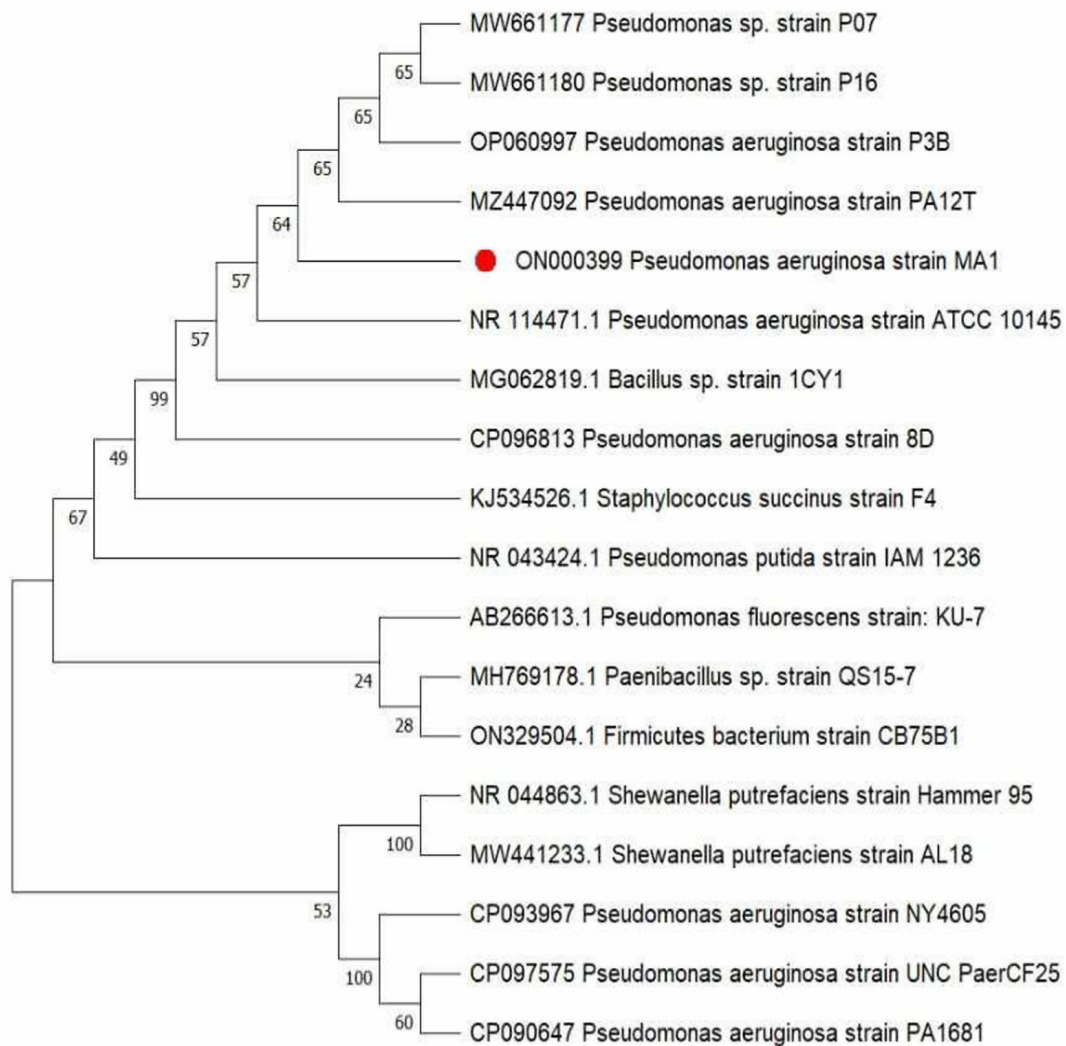


Fig. 3. A neighbor-joining phylogenetic tree of *Pseudomonas aeruginosa* strain MA1 (accession number: ON000399), using 16S rRNA gene sequence, with names of related bacterial species

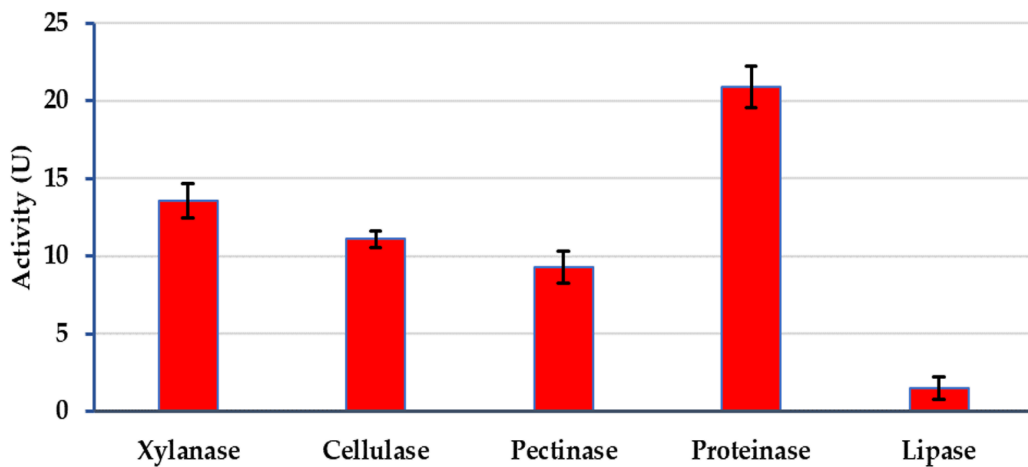


Fig. 4. Hydrolytic enzyme's profile of the isolated bacterial pathogen on common bean tissue [Columns of the enzyme activity are represented as mean \pm SD (n=3)]

TABLE 3. Metabolic changes (mg/g plant fresh weight) in common bean-infected leaves

Treatment	Chlorophyll			Total carotenoids	Proline	Phenolic content	
	a	b	Total			Total	Free
Non-infected control	0.211 ±0.0025 b	0.374 ±0.0040 a	0.248 ±0.0046 a	12.595 ±0.0060 b	0.048 ±0.0031 b	4.709 ±0.0020 b	3.789 ±0.0035 b
Infected plant	0.237 ±0.0031 a	0.283 ±0.0020 b	0.163 ±0.0031 b	13.055 ±0.0031 a	0.088 ±0.0025 a	5.622 ±0.0053 a	5.054 ±0.0025a
T-test (P ≤ 0.05)	0.0114*	0.0002*	0.0012*	0.0000*	0.0002*	0.0000*	0.0000*

Each value represents mean ± standard deviation, n=3

Means of the same parameter with different letters are significantly different (T-test at P ≤ 0.05)

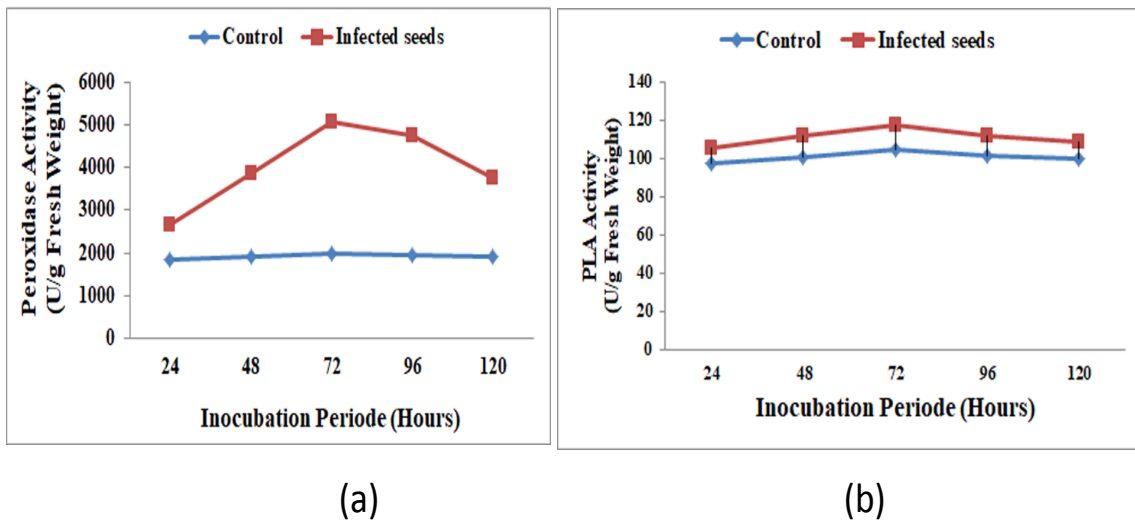


Fig. 5. Time profile of peroxidase and PAL enzyme activity in common bean as a response to infection by *P. aeruginosa* MA1 for five days

Accumulation of PAL transcripts

Foliar artificial infection of common bean leaves with *P. aeruginosa* enhanced significant PAL gene expression, reaching about threefold that of the non-infected corresponding control after 24h of infection (Fig. 6). The transcript abundance decreased in infected leaves, reaching the corresponding control level in the third and fifth days of infection.

Management of P. aeruginosa using Ch-Ag NC

Characterization of Ch-Ag NC

Various methods were used to assess the physicochemical characterization of the synthesized Ch-Ag NC. Figs. 7 A and B indicated that the hydrodynamic diameter was measured in the nm range using the DLS. The size of Ch-Ag NC was 13.27 nm and the zeta potential was +65.6 mV, respectively. Using HR-TEM, we were able to determine the particle size and shape. The Ch-Ag NC was depicted in Fig. 7C in a typical HR-TEM micrograph. The

cross-linking between chitosan and silver has a size range of about 12 nm with a spherical shape and smooth surface. The X-ray diffraction pattern of Ch-Ag NC is shown in Fig. 7D. The peaks at $2\theta = 38.13^\circ, 64.46^\circ, \text{ and } 77.42^\circ$ were assigned to (111), (220), and (311) of Ch-Ag NC, demonstrating that the cubic phase structure of the silver was present in the crystalline structure of the synthesized Ch-Ag NC (JCPDS 04-004-8730). Figure 7E presents the transmittance (%) versus wavenumber (cm^{-1}) plot of the synthesized Ch-Ag NC. Due to the stretching vibrations of the O-H and N-H functional groups, the spectra exhibit a wide absorption band at 3360 cm^{-1} . The spectrum showed N-H and C-N bending vibrations with sharp peaks at 1641 cm^{-1} . Absorption of N-H and C-N originates from the interaction between the metallic surface of silver and the amino group; in such cases the amino groups serve as chelating agents for the stabilization of silver.

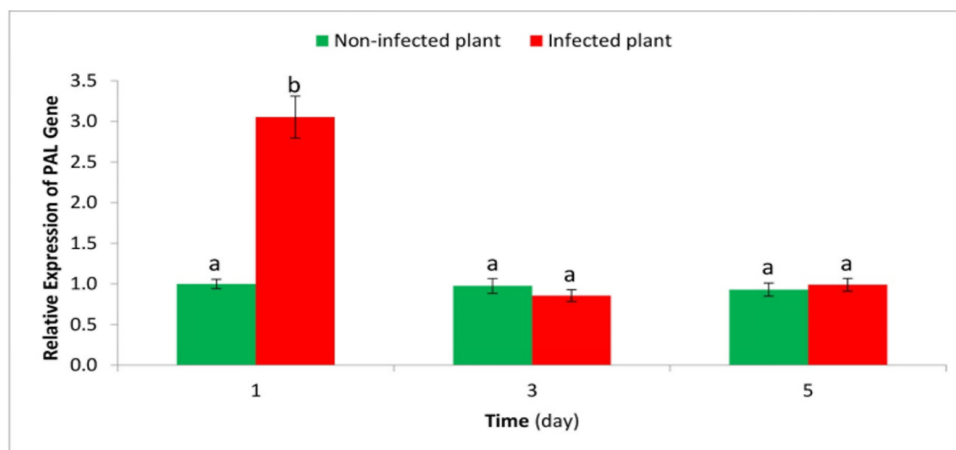


Fig. 6. Regulation of PAL relative expression in common bean was detected by real-time PCR as a response to infection by *P. aeruginosa* MA1 for five days

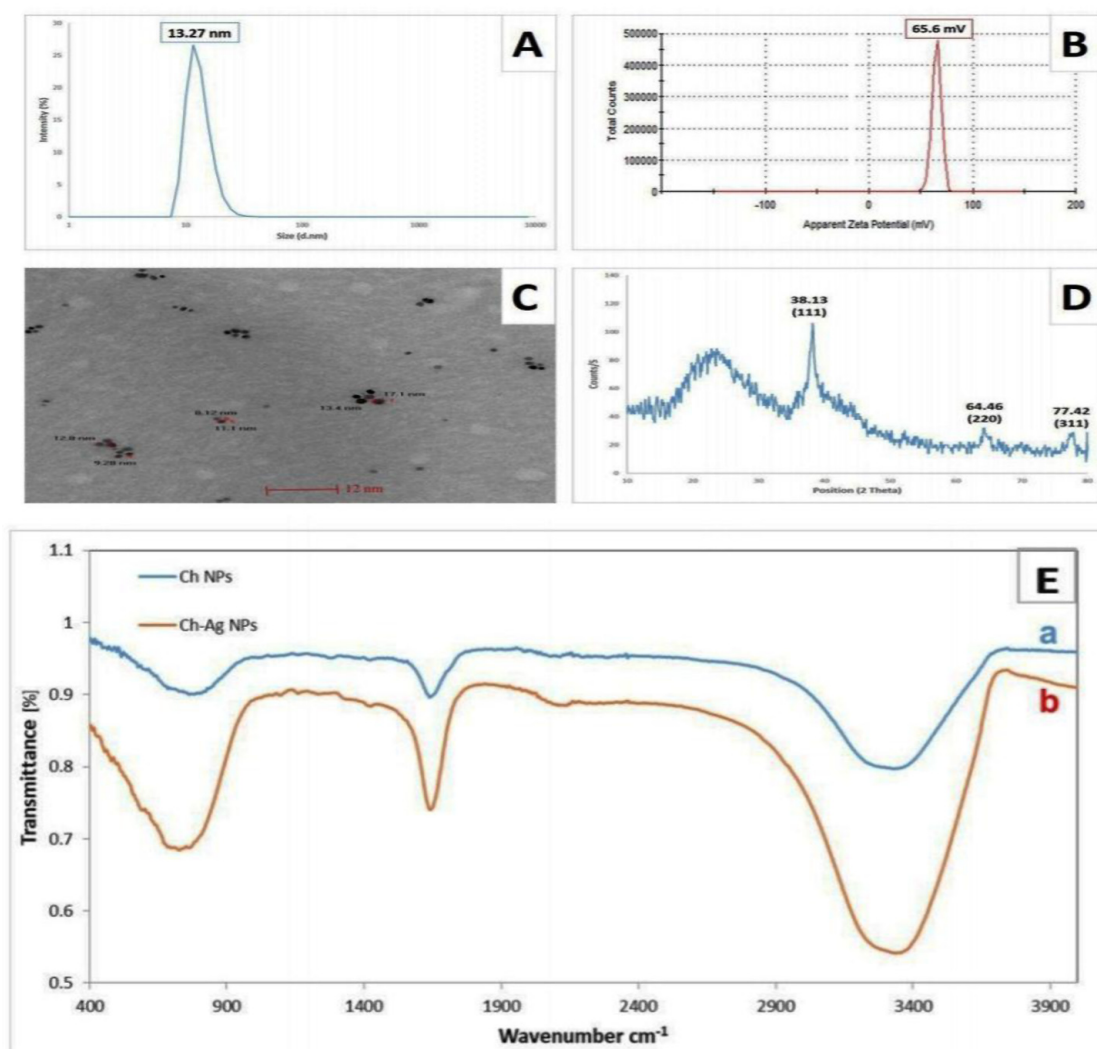


Fig. 7. Characterization of chitosan-silver nanocomposite (Ch-Ag NC). A) Particle size distribution, showing the average size of 13.27 nm; B) Zeta potential, showing the surface charge of +65.6mV; C) HR-TEM image, viewing a spherical shape with a mean size of 12nm; D) XRD pattern analysis suggests the formation of Ch-Ag NC; E). FT-IR spectra of (a) chitosan nanoparticles (Ch NPs) and (b) chitosan-silver nanoparticles (Ch-Ag NC)

In-vitro antibacterial activity of Ch-Ag NC

The antibacterial feature of Ch-Ag NC showed high potential against *P. aeruginosa* strains that manifested through the development of growth inhibition zones (Table 4). It was found that low concentrations of Ch-Ag NC (5, 10, 20, 30, and 40mg/L) had no obvious effect on bacterial growth, but with the increase in nanocomposite concentration to 50 and 100 mg/l, bacterial growth was inhibited. The concentration of 50mg/L was considered the minimum inhibitory concentration (MIC), the lowest concentration that inhibited visible bacterial growth. In addition, it had a clear zone diameter of 1.37 cm compared to the control, which has no clear zone surrounding it (Fig. 8).

TABLE 4. Antibacterial activity of different concentrations of Ch-Ag NC against *P. aeruginosa* strain using an agar-well diffusion assay

Ch-Ag NC (mg/L)	Inhibition zone diameter (cm)
0.0	0.00±0.00 c
5.0	0.00±0.00 c
10.0	0.00±0.00 c
20.0	0.00±0.00 c
30.0	0.00±0.00 c
40.0	0.00±0.00 c
50.0	1.37 ±0.05 b
100.0	2.10 ±0.29 a

All values were represented as mean ±SD, n=3. The values of different letters are significantly different (Tukey test at $P \leq 0.05$).

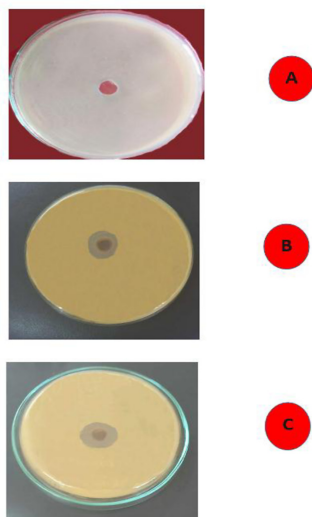


Fig. 8. Antibacterial activity of different concentrations of Ch-Ag NC against *P. aeruginosa*, control (A), 50mg/L (B), and 100mg/L (C)

In-vivo control of *P. aeruginosa* MA1 using Ch-Ag NC

The antibacterial potential of synthesized Ch-Ag NC (50 and 100mg/L) was studied by focusing on the vegetative growth properties of common bean seedlings under the infection stress with MA1. Under infection stress, shoot length showed the lowest value (42.23%) compared to the negative control, and it increased significantly with the application of Ch-Ag NC (50 and 100mg/L) being 80 and 86.6%, respectively. In the same manner, root length showed the lowest value (66.74%) under the infection stress and it increased significantly with the application of Ch-Ag NC (50 and 100mg/L) being 102.11 and 97.89%, respectively. In addition, treatment of seeds with Ch-Ag NC (positive control) improves seedling growth properties. The positive influence of Ch-Ag NC (50 and 100mg/L) recorded the highest shoot length value being 113.6 and 119.88 % respectively, in relation to the negative control. Similarly, root length increased with the application of nanocomposite, recording 101.05 and 105.26 %, as listed in Table 5 and illustrated in Fig. 9.

Discussion

The climatic changes lead to the appearance of new phytopathogens that may be more severe than the already-known ones; further, some pathogens may extend their host range to infect other plants; this, in turn, forces researchers to discover newly adapted phytopathogens. The current study on the common bean is an example of this situation, where it is a universally valuable crop and essential for human nutrition as a grain legume.

Pseudomonas members live as plant associates or parasites. The parasitic species may live on the surface or inside plant tissue, causing diseases that are influenced by ecological aspects and host-specific interfaces (Preston, 2004). Very little consideration has been paid to *Pseudomonas aeruginosa* as one of the causal organisms of soft rot disease in some vegetables and ornamental crops. The current study reported *P. aeruginosa* as a phytopathogen associated with common bean seeds. The bacterial pathogen was identified based on phenotypic characters, biochemical tests, and molecular analysis of the 16S rRNA gene.

TABLE 5. Influence of Ch-Ag NC application on seedling's growth properties in the presence and absence of infection stress

Treatment		Shoot length (cm)	Root length (cm)	Number of rootlets
Negative control	Without any treatment	20.88 ± 2.34 bc	4.75 ± 0.87 b	15.33 ± 2.08 ab
	Ch-Ag NC (50mg/L)	23.72 ± 1.49 ab	4.80 ± 0.46 ab	16.33 ± 1.67 a
Positive control	Ch-Ag NC (100mg/L)	25.03 ± 1.66 a	5.00 ± 1.00 a	15.00 ± 2.65 ab
	MA1 (10 ⁶ cfu/mL)	8.83 ± 0.94 e	3.17 ± 0.35 c	5.23 ± 0.50 d
Ch-Ag NC (50 mg/l) + MA1 (10 ⁶ cfu/mL)		16.70 ± 1.13 d	4.85 ± 0.35 ab	11.00 ± 1.41 c
Ch-Ag NC (100 mg/l) + MA1 (10 ⁶ cfu/mL)		18.09 ± 1.32 cd	4.65 ± 0.95 b	10.02 ± 0.45 c

Values were represented as mean ± SD, n=3.

The means of the same parameter with different letters are significantly different (Tukey test at $P \leq 0.05$).

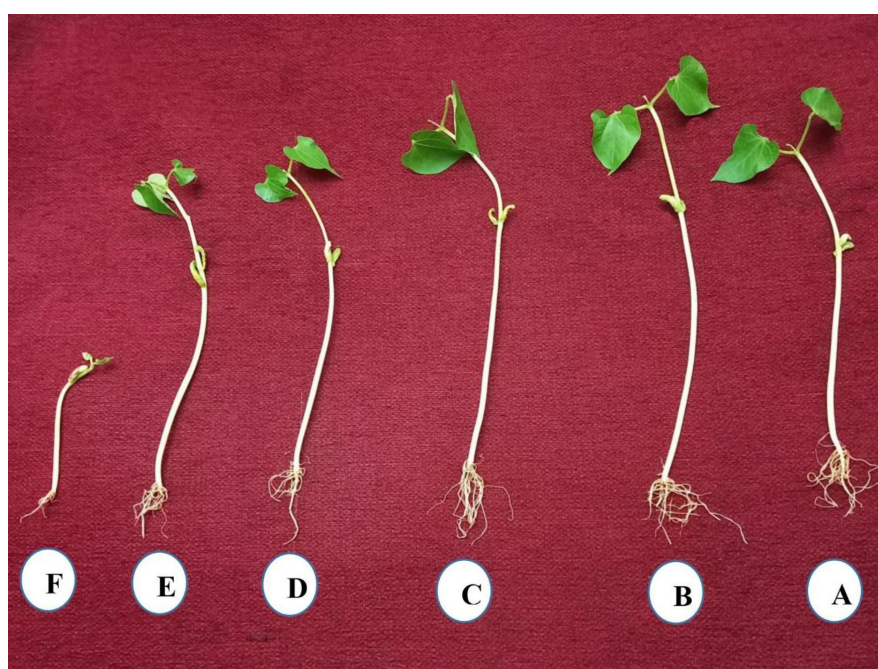


Fig. 9. Growth characteristics associated with the application of two different concentrations of Ch-Ag NC and their antibacterial activity against MA1. Control (A); Ch-Ag NC of 100mg/L (B); Ch-Ag NC of 50mg/L (C); Ch-Ag NC of 100mg/L with bacterial inoculum (D); Ch-Ag NC of 50mg/L with bacterial inoculum (E); Bacterial inoculum of 10⁶ cfu/mL (F)

Seed is the means of plant reproduction and spreading and is a storehouse of food and energy. Plant pathogens are seed transmissible by adhering to the seed surface or becoming internally established within the seed, causing diseases at different stages of plant development, starting from seed germination up to crop maturity, leading to the development of seed and seedling rots, i.e., pre- and post-emergence losses. For example, *P. aeruginosa* suppressed seed germination of *Arabidopsis thaliana* by

releasing a specific molecule (L-2-amino-4-methoxy-trans-3-butenoic acid) that promotes the accumulation of the germination repressors, changing levels of gibberellic acid (GA) which is an essential phytohormone in the germination process (Chahtane et al., 2018). As a model legume, mungbean seeds were infected by a virulent strain of *P. aeruginosa* and showed poor progress of seedling roots and high death rates; further, compared with the wild-type bacterium, the quorum-sensing mutant was notably less virulent (Garge et al., 2018).

The typical identification procedures based on motility, shape, colony color, spore formation, fluorescence, Gram staining properties, and other biochemical tests assumed that the isolated bacterium was *P. aeruginosa*, as previously described (Abd-Alla et al., 2011; Mahmoud et al., 2016). *Pseudomonas aeruginosa* has a uniquely distinctive character: the secretion of a pyocyanin pigment (Garrity et al., 2005) which is a water-soluble blue-green phenazine compound that may have antimicrobial activity and exhibit fluorescence on KB medium under UV light. Pyocyanin biosynthesis, purification, and characterization were reported by Mavrodi et al. (2001) and Mahmoud et al. (2016).

However, to further distinguish the isolated microorganism from the other bacterial species with the same characteristics, 16S rRNA sequencing was accomplished for molecular identification as a sensitive, specific, and rapid method (Moussa et al., 2021). As a result, phylogeny firmly associated the bacterium with closely similar strains and identified the strain as *Pseudomonas aeruginosa*, confirming the previous identification tests.

The 16S rRNA gene was used for molecular identification, and a complete phylogenetic tree was performed. The 1500-bp 16S rRNA gene, which is present in all bacteria, contains DNA sequences that are unique to particular species (Moussa et al., 2022). This aids in identifying the tested bacteria based on their distinctive rRNA gene sequence. *Pseudomonas aeruginosa* was recognized as the pathogenic isolate, and the 16S rRNA sequencing was submitted to GenBank, and assigned the accession number ON000399 to it.

Previously, several soft rot-causative *Pseudomonas* spp. were reported, such as *P. marginalis* on a wide range of plant hosts, including Chinese cabbage, onion, and lettuce, as well as *P. syringae* and *P. marginalis* on onion bulbs in markets and fields (Abd-Alla et al., 2011). Recently, different isolated *Pseudomonas* spp. developed the appearance of water-soaking areas and soft rot symptoms during the infection on different healthy plant tissues, including stems of maize, sweet pepper fruits, eggplant, and tomato (Emami et al., 2018).

In a trial to elucidate the capability of *P. aeruginosa* to invade plant tissue, the enzymatic

profile was assayed against the same plant tissue. The lytic features of the phytopathogen were associated with infection playing a vital role in the disease's progress (Al-Askar et al., 2022a, b). Therefore, the catalytic activity of the current bacterial pathogen was screened on common bean plant tissue. It is already known that the complex nature of plant tissue structure limits the attack of phytopathogens; therefore, some of the cell wall-degrading enzymes (xylanase, cellulase, pectinase, proteinase, and lipase) were assayed, which are supposed to be induced during the infection to enable microbial access into the tissue (Saber et al., 2010; Al-Askar et al., 2021).

Marked xylanase activity was noticed, suggesting the ability of such bacteria to hydrolyze hemicellulose in plant tissue (Abdelwahed et al., 2011; Elsayed et al., 2021; Al-Askar et al., 2022b). Cellulose could also be degraded by cellulase into glucose (Saber et al., 2010; Al-Askar et al., 2022a, b). Pectin is decomposed by pectinase, resulting in monomers of galacturonic acid (Ajayi et al., 2021; Al-Askar et al., 2022a). Furthermore, the proteinaceous tissue is catalyzed by proteases into free amino acids (Al-Askar et al., 2021). Lipase catalyzes the breakdown of triglycerides into free fatty acids, glycerol, diglycerides, and monoglycerides (Saber, 2004). These enzymatic consortiums work synergistically to soften plant tissue, thus easing the invasion process, and therefore, these enzymes pose an additional threat to plant infection. The current *P. aeruginosa* has a complete lytic profile, capable of causing an acute infection.

The metabolic changes in common bean plants associated with infection by *P. aeruginosa* were followed up in terms of chlorophyll (a and b), total carotenoids, proline, and phenolic content (total and free). All such metabolic tests showed significant variation between the infected and healthy groups.

Enhancement of systemically induced resistance is associated with rapid activation of multiple defense mechanisms, which were reported here. The defense mechanisms involve the accumulation of some secondary metabolites, such as proline. As an amino acid, proline contributes to the cell wall structure and is vital to plant growth (Kishor et al., 2015). It was reported to accumulate in infected plants and increase in leaves, thus relating to antioxidant roles by

scavenging the hydroxyl radicals liberated during infection (Verbruggen & Hermans, 2008). Proline also accumulates in the leaf tissues of plants treated with a virulent strains of *P. syringae* but remains unaffected in leaves diseased with isogenic virulent strains, where the virulent strains stimulate the plant defense line as disease resistance (Fabro et al., 2004).

In photosynthetic tissues, carotenoids protect cells from light damage and superoxide radicals. The physiological role of carotenoids is to protect the photosynthetic system against reactive oxygen species (Swapnil et al., 2021). Our data revealed an increase in carotenoids due to infection, suggesting the strong reaction of the common bean against the bacterial pathogen. Likewise, chlorophyll decreased significantly in the stressed crops compared to the control (Mibei et al., 2017). This reaction could also be considered proof of the pathological action of the currently recorded *P. aeruginosa*.

Naturally, many plants synthesize phenolic compounds as a defense line, where they act as free radical scavenging agents and have an antioxidant activity that resists plant infection (Ma et al., 2016). Our tested bacteria trigger the accumulation of phenolic compounds in bean plant tissue, which is consistent with Beimen et al. (1992) who treated tomato plants with three *Clavibacter* strains. Leaf blades showed a reliable accumulation of phenolic compounds depending on time. Similarly, infection of different olive cultivars with *Xylella fastidiosa* subsp. pauca (Xfp), strain CoDiRO, develops leaf scorch symptoms due to the accumulation of phenolic compounds (Luvisi et al., 2017).

A pathogen attack triggers systemic resistance in the host in a series of molecular and metabolic changes in plant tissue. Under the infection with our strain, *P. aeruginosa*, common bean tissue showed a significant rise in the activity of the plant defense-related enzymes POX and PAL, reaching their maximum value at 72 hours of infection. Consequently, POX belongs to oxidoreductases, which elicit the biosynthesis of different secondary metabolites such as lignin and oxidizes phenolic compounds into quinines that protect the plant against pathogen invasion (Reddy et al., 2014; Prasannath, 2017). Moreover, PAL is the precursor of phytoalexin biosynthesis by catalyzing the conversion of L-phenylalanine

to trans-cinnamic acid and ammonia in the phenylpropanoid biosynthetic pathway (Sharma et al., 2018). However, the maximum activity of PAL and POX depends on the difference in cultivar susceptibility and plant age.

Foliar-sprayed common bean plants generated a temporary potentiated defense-related PAL gene expression in 24 h post-infection that vanished with infection progression. Inoculation of the primary leaves of *Phaseolus vulgaris* with virulent and avirulent isolates of *Pseudomonas savastanoi* pv. *Phaseolicola*, and saprophytic *Pseudomonas fluorescens* led to the accumulation of PAL gene transcripts in bean leaves, starting about 15h after inoculation and increasing up to 24h, then decreasing (Meier et al., 1993). Some barley species contain resistance genes (PM-R genes) that control avirulent strains of *Blumeria graminis* f. sp. *hordei* (Bgh). Quantitative RNA blot analysis of PAL transcripts showed that they increase in the susceptible parent at 0–24h and are suppressed at 36–72h. In resistant plants, PAL transcription differed according to the acting rate of their PM-R genes. PM-R genes indirectly modulate defense response gene transcription by limiting fungal incidence (Kruger et al., 2003). Colonization of common bean roots by rhizobacteria with primed defense capacity is known to stimulate systemic resistance against *P. s. pv. phaseolicola*. In resistant leaves of Rhizobium-treated plants, a high accumulation of PAL transcripts after five days of infection was reported (Diaz-Valle et al., 2019). Based on NCBI and Phytozome databases, the host-pathogen interaction elicits the expression of defense-related genes in higher plants, such as the PAL gene, which was selected as a model to evaluate expression patterns in common bean leaves (Iriti & Faoro, 2007).

Chitosan-silver nanocomposite, as an antimicrobial agent, was used here as a suggested line for managing the new *P. aeruginosa* pathogen. *In-vitro* trial showed that Ch-Ag NC possesses antibacterial activity, with the increase in concentration being between 50 and 100 mg/l, which was ensured by its application in the greenhouse. Nanoparticles have a larger specific area and a high reaction activity, demonstrating a deep impact on many living cells (Negm et al., 2021; El-Naggar et al., 2022).

The proposed inhibition mechanisms of chitosan involve the fact that this particle has a

positive charge that allows its interaction with the negative charges of phospholipid constituents in the cell membrane, which disrupts the membrane or alters its permeability, making cellular contents leak out, ultimately causing cell death (Liu et al., 2001; Fosso-Kankeu et al., 2016). Additionally, chitosan acts as a chelating agent for trace elements, thus preventing their availability for normal microbial growth (Zheng & Zhu, 2003; El-Naggar et al., 2022). Nano-chitosan could pass through cell walls, attach to DNA and/or proteins, and stop the functions of essential proteins and enzymes by inhibiting mRNA synthesis (Yien et al., 2012).

Our experimental results showed increased antimicrobial activity of Ch-Ag NC. This may arise from a high infiltration of the silver component with a subsequent high bactericidal effect on the bacterial cell, suggesting a dual mechanism (the bactericidal effect of nanosilver and the effect of nano chitosan) for the antibacterial activity of Ch-Ag NC (Shinde et al., 2021).

Conclusions

Summing up, it is evident that *Pseudomonas aeruginosa* is a phytopathogenic and seed-transmitted bacteria that infects common bean seeds. It can induce obvious pathogenicity symptoms and provoke defense-related responses, including an increase in the activity of POX and PAL as well as upregulation of the PAL gene. It gives a promising response to Ch-Ag NC treatment, which can underlie future potent management.

Data availability statement: The data are available from the corresponding authors upon request.

Acknowledgments: Marwa S. Fouad would like to dedicate this study to the soul of her father Prof. Dr. Sayed Fouad (Professor of animal physiology) who was the first instructor and who set her on the right path. The working team in this study appreciates Prof. Dr. Nabil Sobhi, Bacterial Diseases Research Department, Plant Pathology Research Institute Agricultural Research Centre, Giza, Egypt, for his support and serious contribution to our work.

Conflicts of Interest: The authors declare no potential conflict of interest for this article's research, authorship, and/or publication.

Authors' contributions: Conceptualization, M.F.

and A.G. All authors contribute in methodology. M.F., W.S., H.M. and H.B. organized the database. M.F., W.S. and H.M. performed the statistical analysis. M.F., W.S., H.M. and K. F. wrote the first draft of the manuscript. M.F. and W.S. wrote the discussion section. H.B. and A.G. contributed to interpretation of data. M.F. and H.B. visualization. supervision, M.F. and W.S.

Ethics approval: Not applicable.

References

- Abd-Alla, M.H., Bashandy, S.R., Ratering, S., Schnell, S. (2011) First report of soft rot of onion bulbs in storage caused by *Pseudomonas aeruginosa* in Egypt. *Journal of Plant Interactions*, **6**(4), 229-238.
- Abdelwahed, N.A.M., El-Naggar, N.E., Saber, W.I.A. (2011) Factors and correlations controlling cellulase-free xylanase production by *Streptomyces halstedii* NRRL B-1238 in submerged culture. *Australian Journal of Basic and Applied Sciences*, **5**, 45-53.
- Ajayi, A.A., Lawal, B., Salubi, A.E., Onibokun, A.E., Oniha, M.I., Ajayi, O.M. (2021) Pectinase production by *Aspergillus niger* using pineapple peel pectin and its application in coconut oil extraction. *IOP Conference Series: Earth and Environmental Science (EES)*, 655-665.
- Al-Askar, A.A., Rashad, E.M., Ghoneem, K.M., Mostafa, A.A., Al-Otibi, F.O., Saber, W.I.A. (2021) Discovering *Penicillium polonicum* with high-lytic capacity on *Helianthus tuberosus* tubers: Oil-based preservation for mold management. *Plants*, **10**, 1-23.
- Al-Askar, A.A., Ghoneem, K.M., Hafez, E.E., Saber, W.I.A. (2022a) A case study in Saudi Arabia: Biodiversity of maize seed-borne pathogenic fungi in relation to biochemical, physiological, and molecular characteristics. *Plants*, **11**, 829-856.
- Al-Askar, A.A., Rashad, E.M., Moussa, Z., Ghoneem, K.M., Mostafa, A.A., Al-Otibi, F.O., Saber, W.I.A. (2022b) A novel endophytic *Trichoderma longibrachiatum* WKA55 with biologically active metabolites for promoting germination and reducing mycotoxinogenic fungi of peanut. *Frontiers in Microbiology*, **13**, 772417-772436.
- Alqahtani, F., Aleanizy, F., El Tahir, E., Alhabib, H.,

- Alsaif, R., Shazly, G., et al. (2020) Antibacterial activity of chitosan nanoparticles against pathogenic *N. gonorrhoea*. *International Journal of Nanomedicine*, **15**, 7877–7887.
- Babu, B., Nair, R.S., Angelo, J.M., Mathai, V., Vineet, R.V. (2017) Evaluation of the efficacy of chitosan-silver nanocomposite on *Candida albicans* when compared to three different antifungal agents in combination with standard irrigation protocol: An ex vivo study. *Saudi Endodontic Journal*, **7**, 87-91.
- Bailey, M.J., Beily, P., Poutanen, K. (1992) Interlaboratory testing and methods for assay of xylanase activity. *Journal of Biotechnology*, **23**, 257-70.
- Bates L., Waldren R.P., Teare I.D. (1973) Rapid determination of free proline for water-stress studies. *Plant and Soil*, **39**, 205-207.
- Beimen, A., Bempohl, A., Meletzus, D., Eichenlaub, R., Barz, W. (1992) Accumulation of phenolic compounds in leaves of tomato plants after infection with *Clavibacter michiganense* subsp. *michiganense* strains differing in virulence. *Zeitschrift für Naturforschung, C*, **47**(11-12), 898-909.
- Boersma, J.G., Conner, R.L., Balasubramanian, P.M., Navabi, A., Yu, K., Hou, A. (2014) Combining resistance to common bacterial blight, anthracnose, and beans common mosaic virus into Manitoba-adapted dry beans (*Phaseolus vulgaris* L.) cultivars. *Canadian Journal of Plant Science*, **94**(2), 405-415.
- Cartwright, R. (2010) Book Reviews: Book Reviews. *Perspect. Public Health*, **130**, 239–239.
- Chahtane, H., Fuller, T.N., Allard, P.M., Marcourt, L., Queiroz, E.F., Shanmugabalaji, V., et al. (2018) The plant pathogen *Pseudomonas aeruginosa* triggers a DELLA-dependent seed germination arrest in *Arabidopsis*. *e-Life*, **7**, 37082-37115.
- Chatterton, S., Balasubramanian, P.M., Ericlson, R.S., Hou, A., McLaren, D.L., Henriquez, M.A., Conner, R.L. (2016) Identification of bacterial pathogens and races of *Pseudomonas syringae* pv. *phaseolicola* from dry beans fields in western Canada. *Canadian Journal of Plant Pathology*, **38**, 41-54.
- Chiniquy, D., Barnes, E.M., Zhou, J., Hartman, K., Li, X., Sheflin, A., Pella, A., et al. (2021) Microbial community field surveys reveal abundant *Pseudomonas* population in *Sorghum* rhizosphere composed of many closely related phenotypes. *Frontiers in Microbiology*, **12**, 598180- 598196.
- Cortes-Monllor, A. (1993) Diseases caused by *Pseudomonas* spp. in some cultivars in Puerto Rico: an updating. *The Journal of agriculture of the University of Puerto Rico (USA)*, **77** (3-4), 207-227.
- Dere, Ş., Güneş, T., Sivaci, R. (1998) Spectrophotometric determination of chlorophyll - a, b and total caretenoid contents of some algae species using different solvents. *Turkish Journal of Botany*, **22**, 13–16.
- Diaz-Valle, A., Lopez-Calleja, A.C., Alvarez-Venegas, R. (2019) Enhancement of pathogen resistance in common beans plants by inoculation with *Rhizobium etli*. *Frontiers in Plant Science*, **10**, 1317-1335.
- El-Naggar, N.E.A., Saber, W.I., Zweil, A.M., Bashir, S.I., (2022) An innovative green synthesis approach of chitosan nanoparticles and their inhibitory activity against phytopathogenic *Botrytis cinerea* on strawberry leaves. *Scientific Reports*, **12**(1), 1-20.
- Elsayed, M.S., Eldadamony, N.M., Alrdahe, S.S.T., Saber, W.I.A. (2021) Definitive screening design and artificial neural network for modeling a rapid biodegradation of date palm fronds by a new *Trichoderma* sp. PWN6 into citric acid. *Molecules*, **26**(16), 5084-5106.
- Emami, P., Mehrabi-Koushki, M., Hayati, J., Aeni, M. (2018) Detection and identification of some *Pseudomonas* species causing soft rot using TUF Gene. *Biological Journal of Microorganisms*, **8**(32), 81-93.
- Fabro, G., Kovács, I., Pavet, V., Szabados, L., Alvarez, M.E. (2004) Proline accumulation and *AtP5CS2* gene activation are induced by plant-pathogen incompatible interactions in *Arabidopsis*. *Molecular Plant-Microbe Interactions*, **17**(4), 343–350.
- FAO (Food Agricultural Organization) (2020) <https://www.fao.org/faostat/en/#data/QCL>.
- Felsenstein, J. (1985) Confidence limits on phylogenies:

- An approach using the bootstrap. *Evolution*, **39**, 783-791.
- Feng, Q., Zhang, Z., Chen, Y., Liu, L., Zhang, Z., Chen, C. (2013) Adsorption and desorption characteristics of arsenic on soils: kinetics, equilibrium, and effect of Fe(OH)₃ colloid, H₂SiO₃ colloid and phosphate. *Procedia Environmental Sciences*, **18**, 26-36.
- Fosso-Kankeu, E., De Klerk, C.M., van Aarde, C., Waanders, F., Phoku, J., Pandey, S. (2016) Antibacterial activity of a synthesized chitosan-silver composite with different molecular weights chitosan against gram-positive and gram-negative bacteria. *Int'l Conf. on Advances in Science, Engineering, Technology & Natural Resources (ICASETNR-16)* Nov. 24-25, (South Africa).
- Garge, S., Azimi, S.H., Diggle, S. P. (2018) A simple mung beans infection model for studying the virulence of *Pseudomonas aeruginosa*. *Microbiology*, **164**(5), 764-768.
- Garrity, G.M., Bell, J.A., Lilburn, T. (2005) *Pseudomonadales* Orla-Jensen 1921, 270AL. In: "Bergey's Manual® Syst. Bacteriol.", pp. 323-442.
- Hepperly, P.R., Sinclair, J.B. (1980) Detached pods for studies of *Phomopsis sojae* pods and seed colonization. *Journal of Agriculture of the University of Puerto Rico*, **64**(3), 330-337.
- Iriti, M., Faoro, F. (2007) Review on innate and specific immunity in plants and animals. *Mycopathologia*, **164**, 57-64.
- ISTA (2007) International Seed Testing Association. International Rules for Seed Testing; International Seed Testing Association. ISTA: Bassersdorf, Switzerland.
- King, E.O., Ward, M.K., Raney, D.E. (1954) Two simple media for the demonstration of pyocyanin and fluorescein. *Journal of Laboratory and Clinical Medicine*, **44**, 301-307.
- Kishor, P.B.K., Kumari, P.H., Sunita, M.S.L., Sreenivasulu, N. (2015) Role of proline in cell wall synthesis and plant development and its implications in plant ontogeny. *Frontiers in Plant Science*, **6**, 1-17.
- Kohler, A., Schwindling, S., Conrath, U. (2002) Benzothiadiazole-induced priming for potentiated responses to pathogen infection, wounding, and infiltration of water into leaves requires the NPR1/NIM1 gene in Arabidopsis. *Plant Physiology*, **128**, 1046-1056.
- Kruger, W.M., Szabo, L.J., Zeyen, R.J. (2003) Transcription of the defense response genes chitinase IIb, PAL and peroxidase is induced by the barley powdery mildew fungus and is only indirectly modulated by R genes. *Physiological and Molecular Plant Pathology*, **63**, 167-178.
- Kumar, R., Münstedt, H. (2005) Silver ion release from antimicrobial polyamide/silver composites. *Biomaterials*, **26**(14), 2081-2088.
- Liu, X.F., Guan, Y.L., Yang, D.Z., Li, Z., Yao, K.D. (2001) Antibacterial action of chitosan and carboxymethylated chitosan. *Journal of Applied Polymer Science*, **79**, 1324-1335
- Luvisi, A., Aprile, A., Sabella, E., Vergine, M., Nicoli, F., Nutricati, E. et al. (2017) *Xylella fastidiosa* subsp. *pauca* (CoDiRO strain) infection in four olive (*Olea europaea* L.) cultivars: Profile of phenolic compounds in leaves and progression of leaf scorch symptoms. *Phytopathologia Mediterranea*, **56**(2), 259-273.
- Ma, D., Li Y., Zhang J., Wang C., Qin H., Ding H., Xie Y., Guo T. (2016) Accumulation of phenolic compounds and expression profiles of phenolic acid biosynthesis-related genes in developing grains of white, purple, and red wheat. *Frontiers in Plant Science*, **7**, 528-538.
- Mahmoud, S.Y., Ziedan, E.S.H., Farrag, E.S., Kalafalla, R.S., Ali, A.M. (2016) Antifungal activity of Pyocyanin produced by *Pseudomonas aeruginosa* against *Fusarium oxysporum* schlech a root-rot phytopathogenic fungi. *International Journal of PharmTech Research*, **9**, 43-50.
- Masum, S.M., Ali, M.H., Mandal, M.S.H., Haque, M.N. (2012) Influence of *Parthenium hysterophorus*, *Chromolaena odorata* and PRH on seed germination and seedling growth of maize, soybean and cotton. *Bangladesh Journal of Weed Science*, **3**, 83-90.
- Mavrodi, D.V., Bonsall, R.F., Delaney, S.M., Soule, M.J., Phillips, G., Thomashow, L.S. (2001) Functional analysis of genes for biosynthesis of Pyocyanin and Phenazine-1-Carboxamide

- from *Pseudomonas aeruginosa* PAO1. *Journal of Bacteriology*, **183** (21), 6454–6465.
- Meier, B.M., Shaw, N., Slusarenko, A.J. (1993) Spatial and temporal accumulation of defense gene transcripts in bean (*Phaseolus vulgaris*) leaves in relation to bacteria-induced hypersensitive cell death. *Molecular Plant-Microbe Interactions*, **6**, 453–466.
- Mibei, E.K., Ambuko, J., Giovannoni, J.J., Onyango, A.N., Owino, W.O. (2017) Carotenoid profiling of the leaves of selected African eggplant accessions subjected to drought stress. *Food Science and Nutrition*, **5**(1), 113–122.
- Moghazy, A.M. (2014) Influence of some agricultural practices on seed yield of common beans (*Phaseolus vulgaris*, L.). *Journal of Plant Production, Mansoura University*, **5**(10), 1663–1673.
- Moore, E., Tindall, B., Martins Dos Santos, V., Pieper, D., Ramos, J.-L., Palleroni, N. (2013) Nonmedical: *Pseudomonas*. *Journal of Chemical Information and Modeling*, **53**, 1689–1699.
- Moussa, Z., Darwish, D.B., Alrdahe, S.S., Saber, W.I. (2021) Innovative artificial-intelligence-based approach for the biodegradation of feather keratin by *Bacillus paramycooides*, and cytotoxicity of the resulting amino acids. *Frontiers in Microbiology*, **12**, 731262–731280.
- Moussa, Z., Rashad, E.M., Elsherbiny, E.A., Al-Askar, A.A., Arishi, A.A., Al-Otibi, F.O., Saber, W.I.A. (2022) New strategy for inducing resistance against bacterial wilt disease using an avirulent strain of *Ralstonia solanacearum*. *Microorganisms*, **10**(9), 1814–1835.
- Negm, S., El-Metwally, M., Saber, W.E., Abo-Neima, S., Moustafa, M., El-Kott, A. (2021) Nanoparticles induce the biosynthesis and activity of the new possible therapeutic proteinase source, *Talaromyces purpureogenus* KJ584844. *Biocell*, **45**(1), 119–127.
- Polz, M.F., Cavanaugh, C.M. (1998) Bias in template to product ratios in multitemplate PCR. *Applied and Environmental Microbiology*, **64**, 3724–3730.
- Peralta, H., Aguilar, A., Díaz, R., Mora, Y., Martínez-Batallar, G., Salazar, et al. (2016) Genomic studies of nitrogen-fixing rhizobial strains from *Phaseolus vulgaris* seeds and nodules. *BMC Genomics*, **17**(1), 1–18.
- Preston, G.M. (2004) Plant perceptions of plant growth-promoting *Pseudomonas*. *Philosophical Transactions of the Royal Society B: Biological Sciences*, **359**, 907–918.
- Popovic, T., Milovanovic, P., Aleksic, G., Gavrilovic, V., Starovic, M., Vasic, M., Balaž, J. (2012) Application of semi-selective mediums in routine diagnostic testing of *Pseudomonas savastanoi* pv. phaseolicola on common bean seeds. *Scientia Agricola*, **69**(4), 265–270.
- Prasannath, K. (2017) Plant defense-related enzymes against pathogens: a review. *AGRIEAST: Journal of Agricultural Sciences*, **11**(1), 38–48.
- Reddy, M.S., Ilao, R.I., Faylon, P.S., Dar, W.D., Batchelor, W.D., Sayyed, R., et al. (2014) "Recent Advances in Biofertilizers and Biofungicides (PGPR) for Sustainable Agriculture". Cambridge Scholars Publishing, 510p.
- Saber, W.I.A. (2004) Induced formation and characterization of a lipase produced from *Lactobacillus plantarum* and its uses for hydrolysis of some oils and fats. *Journal of Food and Dairy Sciences*, **29**(12), 7095–7105.
- Saber, W.I.A., El-Naggar, N.E., Abd Al-Aziz, S.A. (2010) Bioconversion of lignocellulosic wastes into organic acids by cellulolytic rock phosphate-solubilizing fungal isolates grown under solid-state fermentation conditions. *Research Journal of Microbiology*, **5**(1), 1–20.
- Saitou, N., Nei, M. (1987) The neighbor-joining method: A new method for reconstructing phylogenetic trees. *Molecular Biology and Evolution*, **4**, 406–425.
- Seevers, P.M., Daly, J.M., Cathedral, F.F. (1971) The role of peroxidase isozymes in resistance to wheat stem rust disease. *Plant Physiology*, **48**, 353–360.
- Seleim, M.A., Abo-Elyousr, K.A., Mohamed, A.A.A., Al-Marzoky, H.A. (2014) Peroxidase and polyphenoloxidase activities as biochemical markers for biocontrol efficacy in the control of tomato bacterial wilt. *Plant Physiology & Pathology*, **2**, 8–11.
- Sharma, N., Pant, B.D., Mathur, J. (2018) *Fusarium oxysporum* induced defense response in resistant and susceptible cultivars of *Eruca sativa* (Miller).

- International Journal of Agricultural Research*, **13**(1), 26-38.
- Shinde, S., Folliero, V., Chianese, A., Zannella, C., De Filippis, A., Rosati, L., et al. (2021) Synthesis of chitosan-coated silver nanoparticle bioconjugates and their antimicrobial activity against multidrug-resistant bacteria. *Applied Sciences*, **11**(19), 9340-9358.
- Snell, F.D., Snell, C.T. (1953) "*Colorimetric Methods of Analysis Including Some Turbidimetric and Nephelometric Methods*." D. Van Nostrand Co., Inc., Princeton, Jersey, Toronto, New York and London, 606p.
- Swapnil, P., Meena, M., Kumar Singh, S., Praveen Dhuldhaj, U., Harish Marwal, A. (2021) Vital roles of carotenoids in plants and humans to deteriorate stress with its structure, biosynthesis, metabolic engineering and functional aspects. *Current Plant Biology*, **26**, 100203-100314.
- Tamura, K., Stecher, G., Kumar, S. (2021) MEGA 11: Molecular Evolutionary Genetics Analysis Version 11. *Mol. Biol. Evol.*, **38**, 3022-3027.
- Tuon, F.F., Dantas, L.R., Suss, P.H., Tasca Ribeiro, V.S. (2022) Pathogenesis of the *Pseudomonas aeruginosa* biofilm: A review. *Pathogens*, **11**(3), 300.
- Verbruggen, N., Hermans, C. (2008) Proline accumulation in plants: A review. *Amino Acids*. **35**, 753-759.
- Walker, T.S., Bais, H.P., Deziel, E., Schweizer, H.P., Rahme, L.G., Fall, R., Vivanco, J.M. (2004) *Pseudomonas aeruginosa* plant root interactions, pathogenicity, biofilm formation, and root exudation. *Plant Physiology*, **134**(1), 320-331.
- Waller, J.M., Lenne, J.M., Waller, S.J. (Eds.) (2002) "*Plant Pathologist's Pocketbook*". (No. 632.3/W198). 3rd edn. CABI Publishing, New York. p.27.
- Wang, L.S., Wang, C.Y., Yang, C.H. (2015) Synthesis and anti-fungal effect of silver nanoparticles-chitosan composite particles. *International Journal of Nanomedicine*, **10**, 2685-2696.
- Wolf, C.E., Gibbones, W.R. (1996) Improved method for quantification of the bacteriocin nisin. *Journal of Applied Bacteriology*, **80**, 453-457.
- Young, J.M., Park, D.C. (2007) Probable synonymy of the nitrogen-fixing genus *Azotobacter* and the genus *Pseudomonas*. *International Journal of Systematic and Evolutionary Microbiology*, **57**, 2894-2901.
- Yien, L., Zin, N.M., Sarwar, A., Katas, H. (2012) Antifungal activity of chitosan nanoparticles and correlation with their physical properties. *International Journal of Biomaterials*, Volume 2012, Article ID 632698, 9 pages
- Zaiter, H.Z., Coyne, D.P. (1984) Testing inoculation methods and sources of resistance to the halo blight bacterium (*Pseudomonas Syringae* pv. *Phaseolicola*) in *Phaseolus vulgaris*. *Euphytica*, **33**, 133-141.
- Zheng, L.Y., Zhu, J.F. (2003) Study on antimicrobial activity of chitosan with different molecular weights. *Carbohydrate Polymers*, **54**, 257-530.
- Zhou, J., Bruns, M.A., Tiedje, J.M. (1996) DNA recovery from soils of diverse composition. *Applied Environmental Microbiology*, **62**, 316-322.
- Zucker, M. (1965) Induction of phenylalanine deaminase by light and its relation to chlorogenic acid synthesis in potato tuber tissue. *Plant Physiology*, **40**, 779-784.

الأدلة الأيضية و الجزيئية للكشف عن بكتيريا *Pseudomonas aeruginosa* الممرضة لبذور الفاصوليا و مكافحتها باستخدام المترابك النانوي للشيتوزان و الفضة

مروة سيد فؤاد^(1,2)، وسام الدين إسماعيل صابر⁽²⁾، هدى حسين بدر⁽³⁾، هشام عبد المنعم محمد⁽¹⁾، خالد يحيى فروح⁽⁴⁾، احمد جمعه⁽³⁾

⁽¹⁾قسم بحوث أمراض البذور- معهد بحوث أمراض النباتات- مركز البحوث الزراعية - الجيزة - مصر،
⁽²⁾وحدة النشاط الميكروبي بقسم الميكروبيولوجي- معهد بحوث الأراضي والمياه والبيئة - مركز البحوث الزراعية- الجيزة - مصر، ⁽³⁾ قسم بحوث الأمراض البكتيرية - معهد بحوث أمراض النباتات- مركز البحوث الزراعية - الجيزة- مصر، ⁽⁴⁾المعمل المركزي للنانوتكنولوجي و المواد المتقدمة بمركز البحوث الزراعية - الجيزة- مصر.

اثبتت هذه الدراسة قدرة مرضية جديدة للمسبب المرضي *Pseudomonas aeruginosa* (MA1) على بذور الفاصوليا مما يسبب التعفن الطري للبذور كطريق للعدوى وتم تعريف البكتيريا الممرضة على اساس جزيئي وتسجيلها في GenBank-NCBI بكونه ON000399. ولقد لوحظ النشاط الإنزيمي لكل من xylanase, cellulase, pectinase, proteinase and protease كالتالي 13.054, 11.09, 9.28, 20.90, and 1.47U على التوالي، مما يشير إلى قدرة MA1 على اختراق الأنسجة النباتية بمعدل إصابة 63.25% و شدة مرضية 42.52%. كما أظهرت القياسات الفسيولوجية انخفاضا ملحوظا في محتوى الكلوروفيل مع زيادة في محتوى البرولين والفيثولات في النبات المصاب كما ازداد النشاط الإنزيمي لكلا من peroxidase and phenylalanine ammonia-lyase (PAL) لتصل إلى الحد الأقصى بعد 72 ساعة من العدوى مع زيادة ملموسة في التعبير عن جين PAL بعد 24 ساعة مما يثبت القدرة للإمراضية ل *P. aeruginosa* على الفاصوليا وعلى هذا، فإن لاكتشاف انتقال هذا المرض بالبذور أهمية قصوى في عمل المزيد من الدراسات المستقبلية لتلك البكتيريا الممرضة. و باختبار تأثير المركب النانوي للشيتوزان و الفضة (Ch-Ag NC) في مكافحة الممرض البكتيري MA1 ثبتت فاعليته و التي تم تأكيدها بتطبيق (ChAg NC) في الصوبة بتركيزات (50 و 100 مجم / لتر) بالإضافة لفاعليته في تحسين خصائص نمو الشتلات بصورة كبيرة.